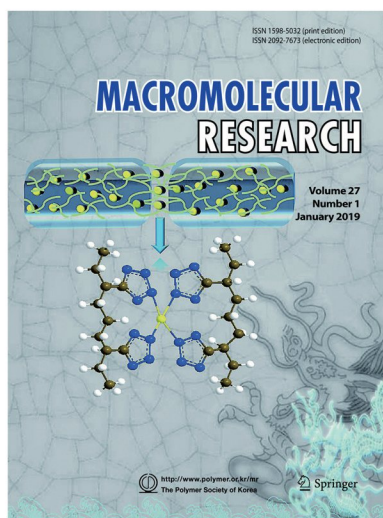


COVER PAPER

Synthesis and Properties of Self-healing Metallopolymers with 5-Vinyltetrazole Units and Zn(II)

Mifa Chen, Wenxiang Wang, Hou Chen*, Liangjiu Bai*, Zhongxin Xue, Donglei Wei, Huawei Yang, and Yuzhong Niu

Vol. 27, No. 1, pp 96-104 (2019) | JAN 25, 2019 | DOI 10.1007/s13233-019-7032-5



The reversible and efficient self-healing metallopolymers were successfully developed by the coordination of tetrazole groups and Zn(II). Polyacrylonitrile-*r*-poly(butyl acrylate) and its subsequent modification were achieved by facile one-pot and two-step methodology. These toughness metallopolymers (MPs) exhibited excellent self-healing properties without complex preparation process and external stimuli at ambient temperature. It can be speculated that the tetrazole-based complex will be widely used in self-healing polymers.

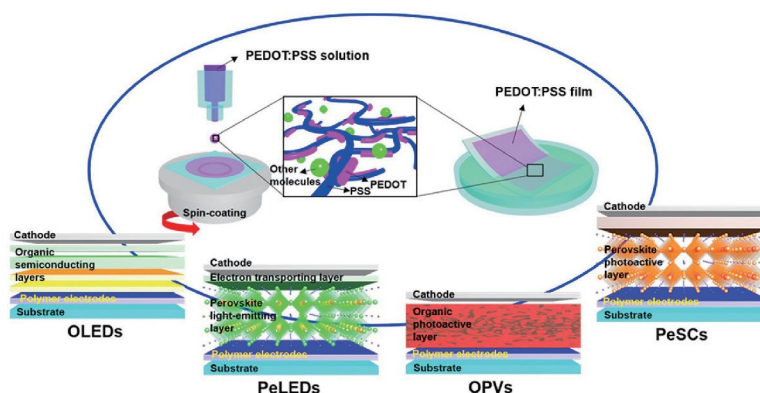
REVIEW

Strategies to Improve Electrical and Electronic Properties of PEDOT:PSS for Organic and Perovskite Optoelectronic Devices

Su-Hun Jeong, Soyeong Ahn, and Tae-Woo Lee*

Macromol. Res., 27, 2 (2019)

Poly(3,4-ethylenedioxythiophene):poly(styrenesulfonate) (PEDOT:PSS) is the most successful commercialized conducting polymer. Many researchers have tried to increase the electrical conductivity, k , of PEDOT:PSS films and apply them to organic and metal halide perovskite optoelectronic devices as transparent electrodes. Recently, the electrical properties of PEDOT:PSS, including k and work function, have been optimized for those optoelectronic devices. Here, we introduce the recent strategies for optimizing the electrical properties of PEDOT:PSS films.



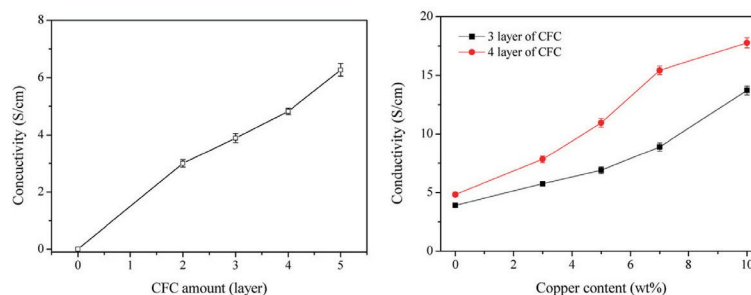
COMMUNICATION

Flexural Properties and Electrical Conductivity of Epoxy Resin/Carbon Fiber Cloth/Metallic Powder Composites

Jie Chen, You-Jia Dong,
Fan-Long Jin*, and Soo-Jin Park*

Macromol. Res., **27**, 10 (2018)

The electrical conductivity of diglycidyl ether of bisphenol A (DGEBA)/carbon fiber cloth (CFC) composites significantly improved with increasing CFC amount and further increased after the addition of metallic powders.



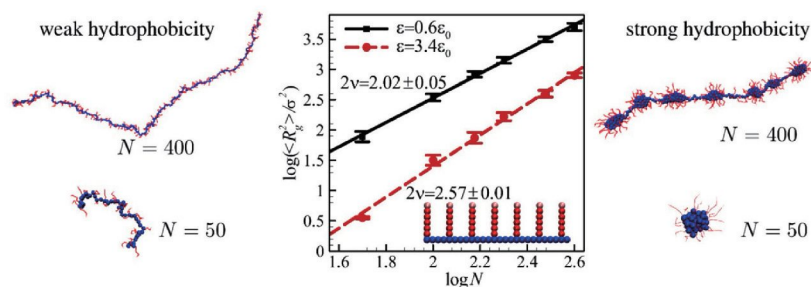
ARTICLES

Single-Chain Conformational Characteristics of Comb-Like Polyelectrolytes: Molecular Dynamics Simulation Study

Soheila Emamyari*
and Hossein Fazli

Macromol. Res., **27**, 14 (2018)

The single-chain conformation of a comb polyelectrolyte was investigated using MD simulations and the effect of some parameters on the conformation of the backbone (R_g) was studied. In addition to R_g , a new parameter (distance profile) was introduced to investigate the backbone conformation in more detail. It was found that ν in $R_g \sim N^\nu$ depends on the hydrophobicity of the backbone (ε). The existence of turn-like segments between successive globular sections leads to much increase of the gyration radius versus N at $\varepsilon=3.4\varepsilon_0$ relative to $\varepsilon=0.6\varepsilon_0$. Hence, the slope increases (to $\nu=1.29$) relative to that for the small value of ε ($\nu=1.01$).

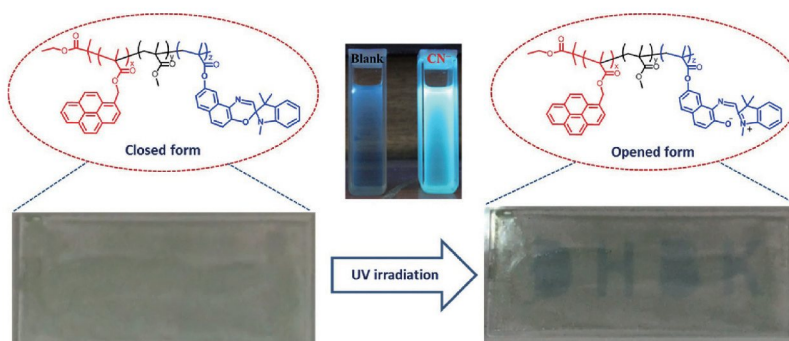


Synthesis of a Novel Fluorescent Cyanide Chemosensor Based on Photoswitching Poly(pyrene-1-ylmethyl-methacrylate-random-methyl methacrylate-random-methacrylate spirooxazine)

Hoan Minh Tran, Tam Huu Nguyen,
Viet Quoc Nguyen, Phuc Huynh Tran,
Linh Duy Thai, Thuy Thu Truong,
Le-Thu T. Nguyen,
and Ha Tran Nguyen*

Macromol. Res., **27**, 25 (2019)

The photo-switching poly(copyrene-1-ylmethyl-methacrylate-random-methyl methacrylate-random-methacrylate spirooxazine) (poly(PyrMMA-*r*-MMA-*r*-MSP)) was successfully synthesized *via* atom transfer radical polymerization with the feed mole ratio of pyrene methacrylate/MMA/MSP comonomers of about 6.5/1/1. Well-defined poly(PyrMMA-*r*-MMA-*r*-MSP) has been obtained with the average molecular weight (M_n) of 7,000 g/mol and polydispersity of 1.23. The well-defined copolymers based on spirooxazine moieties have exhibited the erasable and rewritable photo-imaging on the solid state film which to be as potential candidate for optical data storage materials. Moreover the obtained poly(PyrMMA-*r*-MMA-*r*-MSP) acts as a chemsensor for determination of cyanide ion in solution.

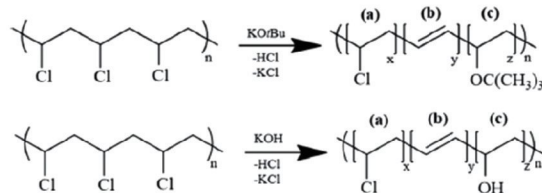


Controlled Dehydrochlorination of Poly(vinyl chloride) for Fabrication of Membranes with Polyacetylene-Like Structure: XPS Analysis and Ion Exchange Membrane Discussion

Eun Ji Park, Seung Yong Lee,
Ali Canlier*, and Taek Sung Hwang*

Macromol. Res., **27**, 33 (2018)

Poly(vinyl chloride) (PVC) membranes were directly dehydrochlorinated by KOTBu and KOH. In this study, competition of elimination and substitution mechanisms were discussed. Also, concept of theoretical ion exchange capacity was suggested for further functionalization.

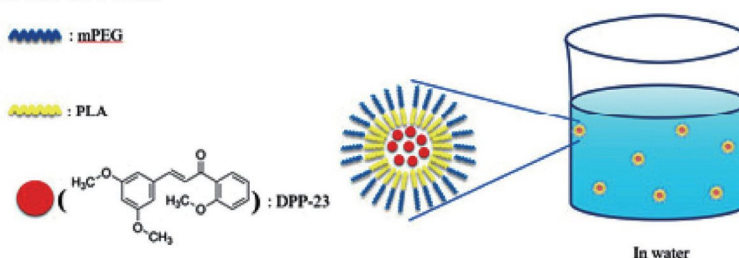


Anticancer Activity of a New Chalcone Derivative-Loaded Polymeric Micelle

Young Jin Kim, Kang Pa Lee,
Do Young Lee, Yun Tae Kim,
Dongsoo Koh, Yoongho Lim,
and Myeong Sik Yoon*

Macromol. Res., **27**, 48 (2018)

A new chalcone derivative-loaded nanoparticle using monomethoxy poly(ethylene glycol)-poly (D,L-lactide) copolymer that tends to spontaneously form micellar formation in aqueous environment shows that it is a reliable drug delivery system by the observation of fluorescein isothiocyanate (FITC) intensity accumulation in MDA-MB-231 cells.

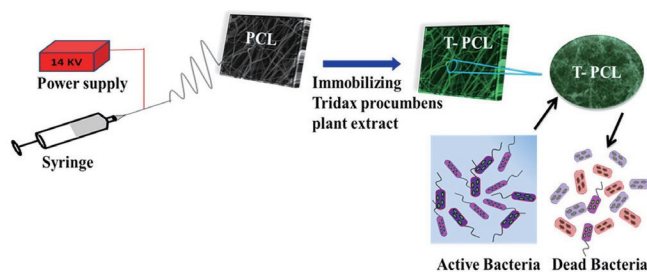


***Tridax Procumbens* Extract Loaded Electrospun PCL Nanofibers: A Novel Wound Dressing Material**

Mathiazhagan Suryamathi,
Chidhambaram Ruba,
Periasamy Viswanathamurthi*,
Velramar Balasubramanian,
and Pachiappan Perumal

Macromol. Res., **27**, 55 (2018)

A novel wound dressing material was developed by immobilizing *Tridax procumbens* plant extract into electrospun polycaprolactone (PCL) nanofibrous scaffold. The antibacterial results of the material shows that the scaffolds act as an enhancer of wound healing and treating surfaces that contain pathogenic microorganisms especially in hospital environment.

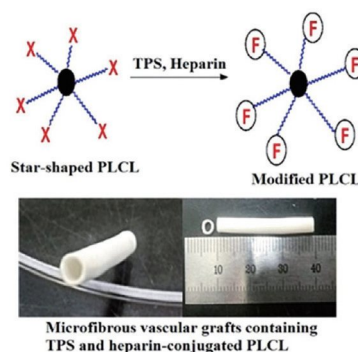


Covalent Immobilization of EPCs-Affinity Peptide on Poly(L-Lactide-co-ε-Caprolactone) Copolymers to Enhance EPCs Adhesion and Retention for Tissue Engineering Applications

Jongyoon Rhee, Muhammad Shafiq,
Donghak Kim, Youngmee Jung,
and Soo Hyun Kim*

Macromol. Res., **27**, 61 (2018)

TPS and heparin were conjugated with star-shaped poly(*L*-lactide-*co*- ϵ -caprolactone) (PLCL) copolymers to simultaneously increase endothelial progenitor cells (EPCs) recruitment and patency of artificial blood vessels. Microfibrillar grafts containing TPS and heparin-conjugated PLCL copolymers were fabricated. Electrospun membranes containing TPS and TPS/Hep facilitated EPCs capture better than did the control group.

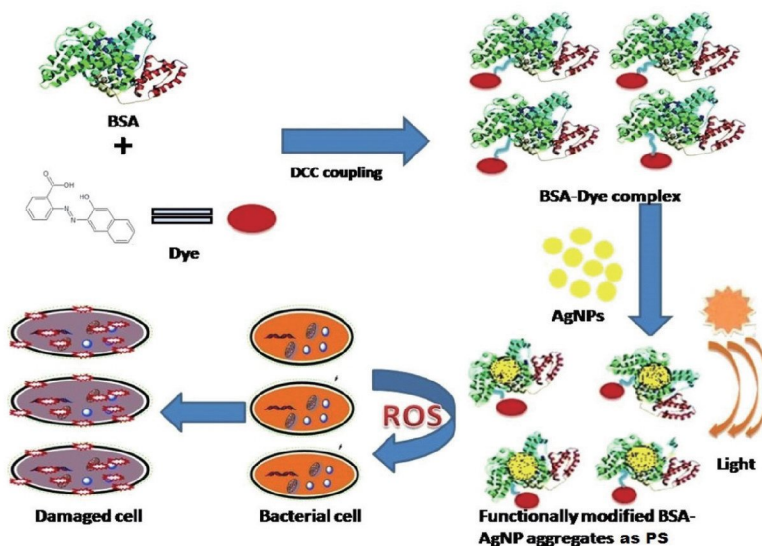


Photochemical Studies and Photoinduced Antibacterial Properties of Silver Nanoparticle-Encapsulated Biomacromolecule Bovine Serum Albumin Functionalised with Photoresponsive Chromophoric System 2-[(E)-(3-Hydroxynaphthalen-2-yl) diazenyl] Benzoic Acid

Lintia Maria Jose
and Sunny Kuriakose*

Macromol. Res., **27**, 73 (2018)

Synthesized silver nanoparticles (AgNP) were stabilized by encapsulating into the scaffold of bovine serum albumin (BSA) functionally modified with photosensitive dye 2-[(E)-(3-hydroxynaphthalen-2-yl) diazenyl] benzoic acid. The optical properties, structural properties, and morphology of the developed system were studied. The antibacterial properties and light induced antibacterial reactivity of the AgNP-BSA-dye system were established. The AgNP encapsulated functionally modified system acquired excellent antibacterial activity that was increased by light irradiation.

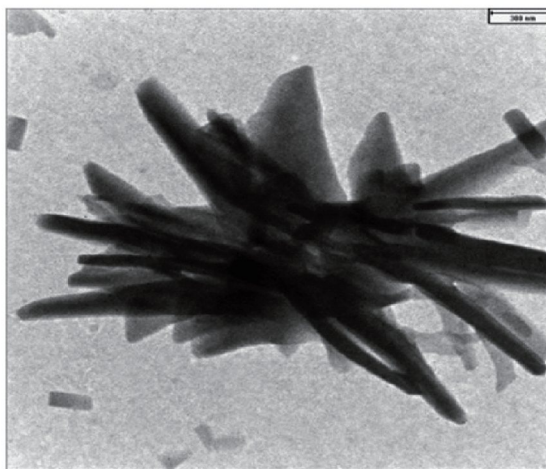


CO₂/N₂ Separation Using Polyvinyl Chloride Iso-Phthalic Acid/Aluminium Nitrate Nanocomposite Membrane

Ehsan Kianfar*, Mahmoud Salimi,
Farshid Kianfar, Mehran Kianfar,
and Seyyed Ali Hasan Razavikia

Macromol. Res., **27**, 83 (2018)

Transmission electron microscopy (TEM) of iso-phthalic acid/aluminium nitrate nanoparticles. Morphology and surface roughness of the nanocomposite were characterized. As a result, it can be expected that nanocomposite iso-phthalic acid/aluminium nitrate have a remarkable separation effect compared to common non-porous types. CO₂/N₂ permeability increases by increasing the percentage levels of iso-phthalic acid/aluminium nitrate nanoparticles from 0.125 to 0.250 wt% in polyvinyl chloride (PVC) precursor. This increase is due to increased permeability of iso-phthalic acid/aluminium nitrate nanoparticles in the polymer network and lack of compatibility of nanoparticle with the polymer caused changes in the intensity of polymer chains and cause the interface between organic polymers and nanoparticles with large surface areas, and in the holes caused by the interface which in general, contribute to an increase in free volume and the area, and these hole areas, are suitable places to absorb and transport of gas molecules through the polymer network. The subsequent diffusion coefficient and permeability increases.

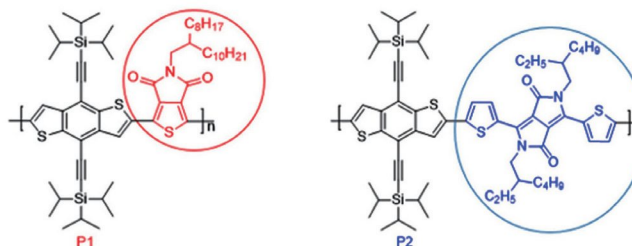


Acceptor Unit Effects for Ambipolar Organic Field-Effect Transistors Based on TIPS-Benzodithiophene Copolymers

Henry Opoku, Chinna Bathula, Melaku Dereje Mamo, Nabeen K Shrestha, Taegweon Lee, and Yong-Young Noh*

Macromol. Res., **27**, 90 (2018)

By varying the acceptor units attached to a Triisopropylsilyl benzo[1,2-b:4,5-b']dithiophene (TIPS-BDT) donor block, two narrow band gap polymers **P1** and **P2** were synthesized and applied for ambipolar organic field effect and complementary optoelectronic properties, with **P1** showing superior performance in transistor and inverter applications.

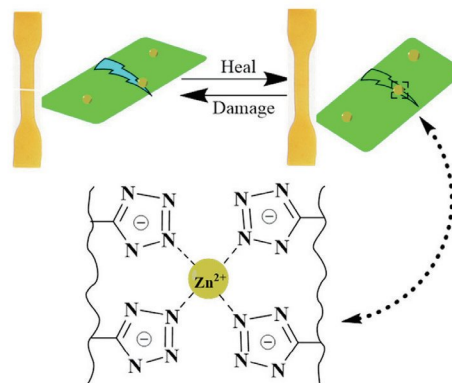


Synthesis and Properties of Self-healing Metallopolymers with 5-Vinyltetrazole Units and Zn(II)

Mifa Chen, Wenxiang Wang, Hou Chen*, Liangjiu Bai*, Zhongxin Xue, Donglei Wei, Huawei Yang, and Yuzhong Niu

Macromol. Res., **27**, 96 (2019)

Polyacrylonitrile-based copolymers were rapidly synthesized and modified by one-pot method. Zinc chloride (ZnCl_2) was used as catalyst to modify cyano groups and coordinate with the generated tetrazole groups for highly self-healing performance. This simple and efficient preparation process of excellent self-healing materials will provide a green route of potential applications.



Cover Paper

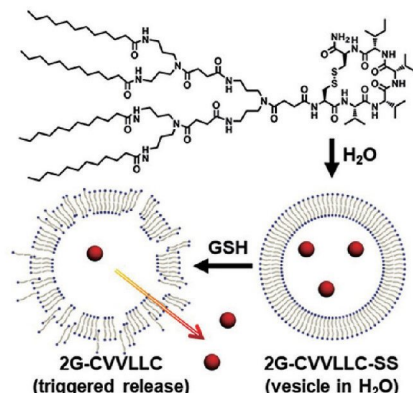
NOTE

Stimuli-Responsive Structural Transformation of Self-Assembled Dendron-Peptide Conjugate and Its Triggered Cargo Release

Jeonghun Lee, Eunbyeol Noh, and Chulhee Kim*

Macromol. Res., **27**, 105 (2019)

Introduction of peptides at the focal point could provide dendrons with unique properties. We prepared dendron-peptide conjugate consist of second generation amide dendron and CVVLLC peptide with intramolecular disulfide bond (2G-CVVLLC-SS). 2G-CVVLLC-SS self-assembled into a vesicular structure in aqueous phase. Upon the addition of a reducing agent into the vesicular solution containing SRB dye, the entrapped cargo was released in a controlled manner by structural transformation from a vesicle (2G-CVVLLC-SS) to an irregular structure (2G-CVVLLC). Therefore, this stimuli-responsive structural transformation of dendron-peptide conjugate using intramolecular disulfide bond would be valuable for preparation of self-assembled structure with triggered cargo release property.

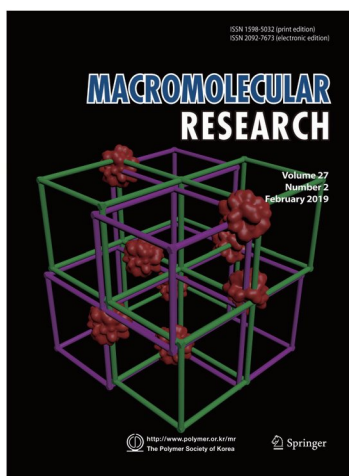


COVER PAPER

Interpenetrating Polymer Network Hydrogels of Gelatin and Poly(ethylene glycol) as An Engineered 3D Tumor Microenvironment

Dong Shin Lee, Jeon Il Kang, Byeong Hee Hwang*, and Kyung Min Park*

Vol. 27, No. 2, pp 205-211 (2019) | FEB 25, 2019 | DOI 10.1007/s13233-019-7072-7



The interpenetrating polymer network (IPN) hydrogels were successfully developed *via* horseradish peroxidase-mediated dual cross-linking reactions. The IPN hydrogels exhibited independently controllable physicochemical properties, resistance to the proteolytic enzymes, and cytocompatibility for a long-term culture of cancer cells. Also, we utilized the engineered tumor construct as a platform to evaluate the effect of matrix stiffness on cancer cell proliferation and drug resistance. In conclusion, we suggest that our IPN hydrogel is a promising material to study cancer biology and to screen innovative therapeutic agents for better clinical outcome.

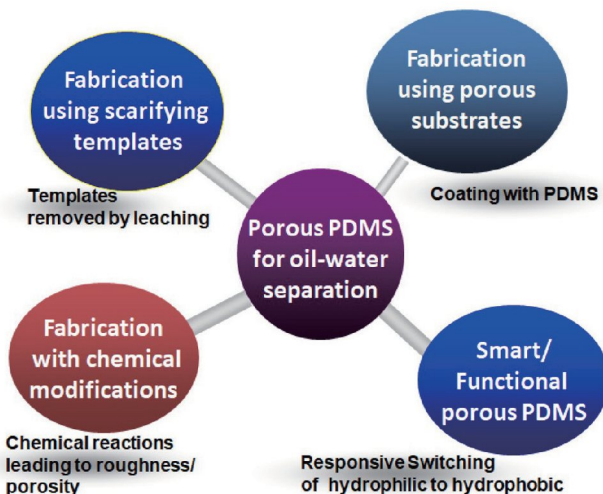
REVIEW

Strategies for Fabrication of Hydrophobic Porous Materials Based on Polydimethylsiloxane for Oil-Water Separation

Kantappa Halake, Soomin Bae, Jiyoung Lee, Yunho Cho, Hongil Jo, Jowoong Heo, Kyungtae Park, Hyeongju Kim, Hyun Ju, Yongkyun Kim, Amirhosseini Hasani, Thuy Duong Pham, Jaeho Choi, Sohyeon Hong, Seongcheol Choi, and Jonghwi Lee*

Macromol. Res., 27, 109 (2019)

The separation of organic contaminants from industrially produced wastewater is a serious environmental challenge, and the preparation of superior oil absorbents is critical for overcoming this challenge. This article reviews the recent progress in the fabrication of porous polydimethylsiloxane (PDMS) materials, which are the most widely investigated materials for oil-water separation.



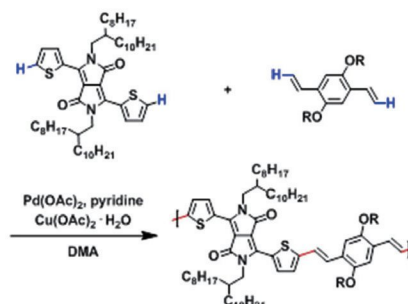
COMMUNICATION

Synthesis and Characterization of DPP-Based Conjugated Polymers via Dehydrogenative Direct Alkenylation Polycondensation

Jiwon Lee, Hea Jung Park,
Jung Min Joo, and Do-Hoon Hwang*

Macromol. Res., **27**, 115 (2019)

Two new π -conjugated polymers were synthesized by polycondensation via dehydrogenative direct alkenylation using the $\text{Pd}(\text{OAc})_2/\text{pyridine}$ catalyst without directing groups. The C-H activation of the C-5 position on the thiophene moiety of 3,6-di(thiophen-2'-yl)diketopyrrolopyrrole derivative occurred readily, giving regioselective cross-coupled products in *trans*-configuration. The optical, electrochemical, and thermal properties of the synthesized polymers were also investigated.



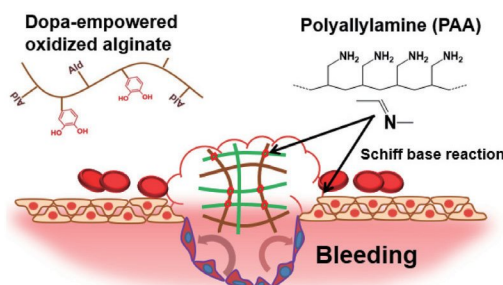
ARTICLES

Dopa-Empowered Schiff Base Forming Alginate Hydrogel Glue for Rapid Hemostatic Control

Chung Kil Song, Min-Kyoung Kim,
Junghan Lee, Enkhzaya Davaa,
Rengarajan Baskaran,
and Su-Geun Yang*

Macromol. Res., **27**, 119 (2019)

Dopa-OA glue is quickly formed hydrogel within 5 to 10 seconds after mixing dopamine-conjugated oxidized alginate with polyallylamine and successfully stop the bleeding on wound tissue through the Schiff base reaction and dopa quinone reaction. In addition, Dopa-hemostatic glue is easily not detached from wound tissue by the elastic and mussel-pad like adhesive property of Dopa.

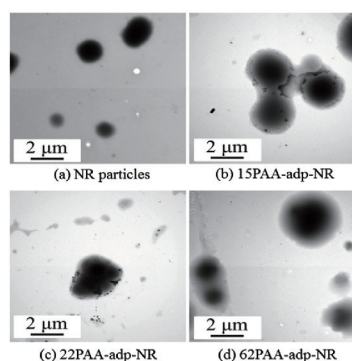


Polymer Electrolyte from Natural Rubber-Polyacrylic Acid and Polypyrrole and Its Application

Pensiri Silakul
and Rathanawan Magaraphan*

Macromol. Res., **27**, 126 (2019)

The core-shell of polyacrylic acid (PAA) coated on natural rubber (NR) surface was successfully synthesized by using admicellar polymerization. The results showed that the thickness of PAA-adp-NR increased with increasing AA monomer content. The PAA shell content was the highest at 62PAA-adp-NR causing the good affinity between PAA and liquid electrolyte to form polymer gelation. The incorporation of PAA enhanced the ionic conductive pathway and showed a potential for using in dye sensitized solar cells (DSSCs). The long-term stability of PAA-adp-NR was improved by chemical crosslink. Additionally, the electron conductivity and solar conversion efficiency were significantly increased by incorporated PPy into PAA-adp-NR and crosslinked PAA-adp-NR.

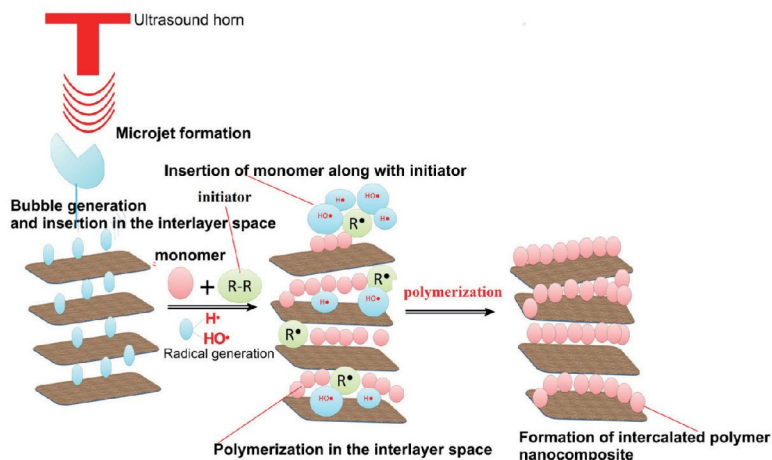


Synthesis, Characterization and *in vitro* Drug Release Studies of Sonolytically Intercalated Poly(*o*-anisidine)/Montmorillonite Nanocomposites

Anurakshee Verma
and Ufana Riaz*

Macromol. Res., 27, 140 (2019)

Intercalation and polymerization of poly(*o*-anisidine) in the interlayer space of montmorillonite (MMT) takes place *via* ultrasonic cavitation. When clay particles dispersed in water and exposed to ultrasonic vibrations, alternating expansive as well as compressive acoustic waves create acoustic cavities/bubbles that penetrate into the interlayer space of MMT. This leads to expansion of gallery height. The acoustic bubbles accumulate high ultrasonic energy and subsequently collapse after attaining a critical size, thereby releasing the energy stored in the bubble which is utilized by the monomer and the initiator present in the reaction mixture to undergo polymerization. This causes insertion of polymer in the interlayer space of clay.

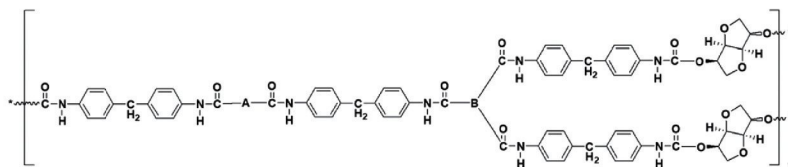


Polymerization Kinetics and Physical Properties of Polyurethanes Synthesized by Bio-Based Monomers

Sun Tae Cho, Jae Il So,
Ji-Young Jung, Sosan Hwang,
Sung-Hyeon Baek,
and Sang Eun Shim*

Macromol. Res., 27, 153 (2019)

The kinetics of polymerization and the properties of polyurethane synthesized from renewable sources such as isosorbide and castor oil were studied in terms of structural, physical, thermal, and morphological properties.



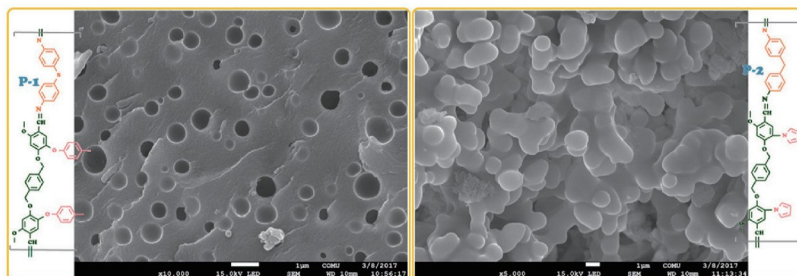
Bio-based polyurethane

Poly(azomethine)s Anchored by Cresol and Pyrrole Units: Synthesis, Characterization and Spectroscopy Studies

İsmet Kaya*, Feyza Kolcu,
Gizem Tasvir Arıcı,
and Ezgi Çölekoğlu

Macromol. Res., 27, 164 (2019)

Incorporation of *p*-cresol and pyrrole as side chain along the poly(azomethine) backbone increases solubility characteristics, without affecting thermal properties. Aromatic polymers containing heterocyclic rings in side chain act as signaling units, due to their fluorescent characteristics. Onset temperature values of poly(azomethine)s containing *p*-cresol (P-1) and pyrrole (P-2) units, were found as 236 and 248 °C, respectively. Synthesized compounds demonstrated multi-chromic properties in DMF solutions.

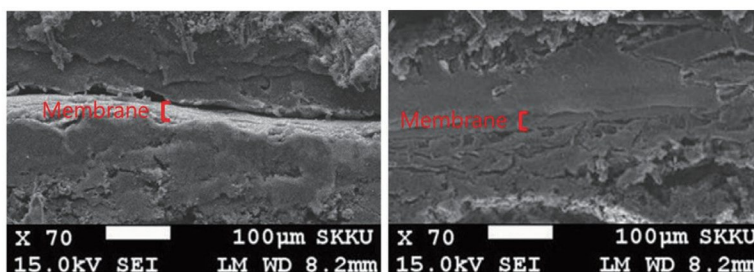


Binder Effect on Fuel Cell Performance and Interfacial Stability of Membrane Electrode Assembly Fabricated with Sulfonated Poly(ether ether ketone) Membrane

Jongwook Lee, Yeonho Ahn,
and Dukjoon Kim*

Macromol. Res., **27**, 175 (2019)

In this study, sulfonated poly(ether ether ketone) (sPEEK) was prepared as an alternative binder for the Nafion® to increase interfacial stability of membrane-electrode assembly (MEA) fabricated with sPEEK membrane. To analyze the binder effect, MEAs were fabricated with two types of binders, sPEEK 65 and Nafion® ionomer. During the cell operation at the low relative humidity, an interfacial instability was not observed in the MEA with sPEEK binder, although MEA with Nafion® binder showed the gap between membrane and catalyst layer.

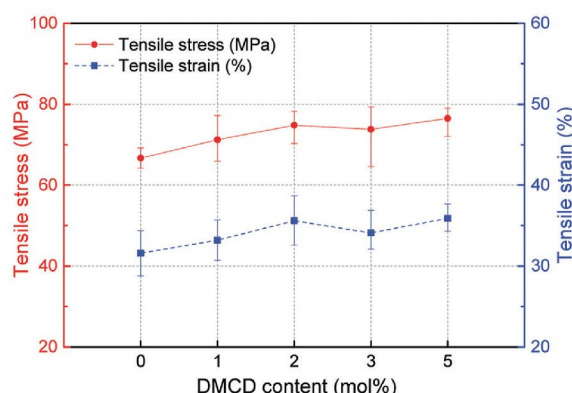


Effect of Dimethyl 1,4-Cyclohexane Dicarboxylate on Mechanical Properties and Crystallization Behavior of Poly(trimethylene Terephthalate) Co-Polymer

Han Na Kim, Daesun Park,
Je Sung Youm, Bookyeong Jang,
and Jeong Cheol Kim*

Macromol. Res., **27**, 182 (2019)

This study investigated the effects of dimethyl 1,4-cyclohexane dicarboxylate (DMCD) on the physical properties of poly(trimethylene terephthalate) (PTT) co-polyesters. A small amount of DMCD was added when manufacturing PTT. The physical properties of the PTT co-polyester significantly changed when the DMCD content reached 2 mol%. The thermal properties remained similar, the crystallization rate increased, and the thermal stability and mechanical properties were significantly improved up to 2 mol%.



Influence of Solution pH on Drug Release from Ionic Hydrogel Lens

Guenhei Kim, Hyeok Jung Kim,
and Hyeran Noh*

Macromol. Res., **27**, 191 (2019)

We fabricated silicone hydrogel contact lenses for drug delivery and determined the mechanism of each drug delivery system. The experimental data for the time-dependent drug release and hydrogel swelling implied evidence for the criteria of the drug diffusion. This study proposes the possibility of controlled drug delivery by silicone hydrogel contact lenses at physiological pH conditions.

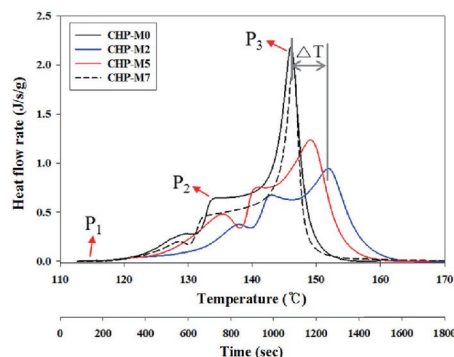


Encapsulation of Peroxide Initiator in a Polyurea Shell: Its Characteristics and Effect on MMA Polymerization Kinetics

Hyeon Jin Kwon, Eun Ju Lee,
Mi Rae Kim, Kang Ho Cheon,
Hee Jung Park, and Kee Yoon Lee*

Macromol. Res., **27**, 198 (2019)

In this study, microcapsules with polyurea shells were prepared from oil-in-water (O/W) emulsion under various agitation speeds (230, 500, and 700 rpm) to encapsulate cumene hydroperoxide (CHP) and tert-butyl peroxy-2-ethyl hexanoate (TBPEH). Thus prepared microcapsule size and shell contents were observed to be decreased upon increasing the agitation speed. Differential scanning calorimetry (DSC) was used to measure and compare the effect on the reaction kinetics of the methyl methacrylate (MMA) radical polymerization in the presence of various initiators. When encapsulated initiator used instead of unencapsulated initiator the maximum conversion and maximum reaction rate were decreased and the reaction temperature was delayed. The delay in reaction temperature was larger as the agitation speed decreased. In the case of encapsulated CHP at 230, 500, 700 rpm, the temperature at the maximum reaction rate was delayed by 5.8, 3.0, and 0.4 °C, respectively, compared to unencapsulated CHP.

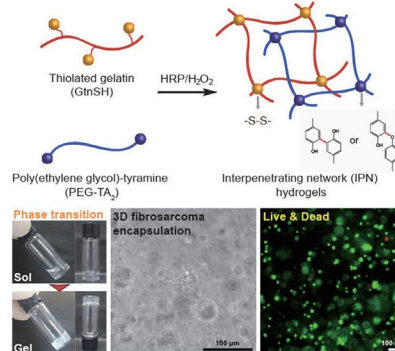


Interpenetrating Polymer Network Hydrogels of Gelatin and Poly(ethylene glycol) as an Engineered 3D Tumor Microenvironment

Dong Shin Lee, Jeon Il Kang,
Byeong Hee Hwang*,
and Kyung Min Park*

Macromol. Res., **27**, 205 (2019)

Although various bio-inspired hydrogel materials have been utilized as engineered tumor models, it is still challenging to develop advanced polymeric hydrogels that can more accurately reconstruct critical aspects of the native tumor microenvironment. Herein, we present interpenetrating polymer network (IPN) hydrogels composed of thiolated gelatin and tyramine-conjugated poly(ethylene glycol), which can be used as an engineered 3D tumor microenvironment to study cancer biology and to screen innovative therapeutic agents for better clinical outcome.



Cover Paper

NOTE

Synthesis of Helical Polyisocyanide with Alkyne End-Group Using Grignard Reaction

Min-soo Cho, Ji-sun Yu,
Jun-hee Cho, Jin-Wook Han,
and Young-Je Kwark*

Macromol. Res., **27**, 212 (2019)

Helical polyisocyanide (PI) with alkyne end groups were prepared by applying Grignard reaction to PI prepared using an organonickel initiator. The organonickel initiator induced living polymerization of 4-methoxyphenyl isocyanide to give polymer chains with nickel bromide end groups, which reacted with the Grignard reagent to introduce alkyne end groups. During the reaction, dimerization of alkyne groups catalyzed by the resulting Ni(0) complex was observed to result in PI with doubled molecular weight. The dimerization could be successfully suppressed by adding additional ligands during the Grignard reaction step.

